

Todralazine Protects Zebrafish from Lethal Effects of Ionizing Radiation: Role of Hematopoietic Cell Expansion

Manali Dimri,¹ Jayadev Joshi,¹ Rina Chakrabarti,² Neeta Sehgal,² Angara Sureshbabu,³ and Indracanti Prem Kumar¹

Abstract

The Johns Hopkins Clinical Compound Library (JHCCL), a collection of Food and Drug Administration (FDA)-approved small molecules (1400), was screened *in silico* for identification of novel β_2 AR blockers and tested for hematopoietic stem cell (HSC) expansion and radioprotection in zebrafish embryos. Docking studies, followed by the capacity to hasten erythropoiesis, identified todralazine (Binding energy, -8.4 kcal/mol) as a potential HSC-modulating agent. Todralazine ($5 \mu\text{M}$) significantly increased erythropoiesis in caudal hematopoietic tissue (CHT) in wild-type and anemic zebrafish embryos (2.33- and 1.44-folds, respectively) when compared with untreated and anemic control groups. Todralazine ($5 \mu\text{M}$) treatment also led to an increased number of erythroid progenitors, as revealed from the increased expression of erythroid progenitor-specific genes in the CHT region. Consistent with these effects, zebrafish embryos, *Tg(cmyb:gfp)*, treated with $5 \mu\text{M}$ todralazine from 24 to 36 hours post fertilization (hpf) showed increased (approximately two-folds) number of HSCs at the aorta-gonad-mesonephros region (AGM). Similarly, expression of HSC marker genes, *runx1* (3.3-folds), and *cMyb* (1.41-folds) also increased in case of todralazine-treated embryos, further supporting its HSC expansion potential. Metoprolol, a known beta blocker, also induced HSC expansion (1.36- and 1.48-fold increase in *runx1* and *cMyb*, respectively). Todralazine ($5 \mu\text{M}$) when added 30 min before 20 Gy gamma radiation, protected zebrafish from radiation-induced organ toxicity, apoptosis, and improved survival (80% survival advantage over 6 days). The 2-deoxyribose degradation test further suggested hydroxyl (OH) radical scavenging potential of todralazine, and the same is recapitulated *in vivo*. These results suggest that todralazine is a potential HSC expanding agent, which might be acting along with important functions, such as antioxidant and free radical scavenging, in manifesting radioprotection.

Introduction

LOW LINEAR ENERGY TRANSFER radiations like gamma and X-rays inflict damage to cells, in a dose-dependent manner, through generation of free radicals and oxidative stress. Radiation can induce acute effects displaying as lethality and long-term effects showing as induction or enhanced sensitivity to a variety of chronic diseases.¹⁻³ At the molecular level, ionizing radiation induces damage to DNA, protein, and lipids leading to downstream stress-related responses, such as cell cycle arrest and apoptosis.⁴ Because of pertinent health concerns in case of a potential radiation exposure scenario, such as terrorist attacks and reactor accidents along with the ever-expanding medical application of radio-

nuclides, the development of clinically acceptable radiation countermeasure agents holds strategic importance.² Several synthetic and natural compounds by themselves, or in combination, exert protection against lethal doses of ionizing radiation to a variety of models.⁵ Among others, the different mechanisms attributed for radioprotection include free radical scavenging, antioxidant, and metabolic modification.⁶ However, a clinically acceptable agent for protection against lethal doses of ionizing radiation is still eluding. Bone marrow transplantation has been the part of the first line of defense for management of radiation overexposed victims. The pioneering work by Lorenz *et al.* has proved that transplantation or shielding of blood-forming tissues was enough for achieving protection against lethal doses of ionizing radiation.⁷

¹Radiation Biosciences Division, Institute of Nuclear Medicine and Allied Sciences, Defense Research and Development Organization, Delhi, India.

²Department of Zoology, Delhi University, Delhi, India.

³Department of Pediatrics, Yale University, New Haven, Connecticut.

Furthermore, transplantation of hematopoietic stem cells (HSCs) is sufficient for survival against radiation-induced lethality. Stem cells are characterized by their capacity to self-renew and differentiate into progressively restricted cells with specific cell fate. It is well understood that agents that expand HSCs have potential applications to manage life-threatening diseases, including radiation overexposed victims.^{8,9} In view of the promising therapeutic advantages that hematopoietic stem cells (HSCs) hold, efforts are on to identify agents that expand hematopoietic stem and progenitor cells (HSPCs) both *in vivo* and *ex vivo*.⁹

Molecules of both synthetic and natural origin are known to expand HSCs *ex vivo* and *in vivo* and the important ones include prostaglandin E2,¹⁰ stem regenin1,¹¹ and garcinol.¹² Previously, chemically diverse small molecules have been reported to exert HSC expansion and among them β_2 AR antagonist was one of the promising categories.¹³ The search for identifying better drug targets and agents for HSC expansion using the small-molecule library, combinatorial chemicals, and collection of lead-like molecules is under active investigation.^{9,10,12,13} However, a novel molecule identified from the screen needs to undergo the compulsory clinical trials before human applications. Because of the high attrition in a phase I clinical trial, routine drug discovery programs suffer money and time loss.¹⁴ In view of this, drug repurposing or repositioning is a promising approach with high translatability.¹⁴ Important success stories, including novel applications for thalidomide, fluoxetine, etc., have renewed interest in identifying leads for other important human diseases.¹⁴ Screening of the small-molecule clinical compound library for identification of novel molecules with radioprotective action has promising translatability.^{14,15} Target-based screening of large collections of compounds, using cell lines (*in vitro*) as a model system, yielded molecules with potential therapeutic implications. However, cell lines do not mimic the physiological context and, importantly, in the neuroendocrine context, which significantly dictates success in preclinical and clinical stages. Mice are a valuable model system for understanding the pathophysiology of human diseases. However, the size, labor, and time needed make it cost prohibitive for conducting small-molecule screens. Therefore, there is a compelling need for identifying novel animal models, which satisfy the *in vivo* context and high- or medium-throughput screening. Over the past three decades, the zebrafish has made a significant impact in biomedical research and it has been used to study issues of biomedical significance.^{16,17} High fecundity, lesser husbandry cost with advantages like rapid development, availability of genetic resources, ease of the development of transgenic lines, and amenability for medium-throughput screening has made this tropical tiny teleost a valuable model organism.^{18–20} Comparison of zebrafish and human reference genome indicates that 70% of human genes have at least one zebrafish orthologue.²¹ Developing and adult zebrafish have also been used for screening and identification of radioprotectors.^{22–24} In view of the importance that HSCs hold in the management of radiation overexposed victims, the present study aims at screening the Johns Hopkins Clinical Compound Library (JHCCL)²⁵ for identification of novel β_2 AR antagonists with HSC expanding agents. Furthermore, the novel hits were tested for radioprotection using the developed zebrafish embryo as a model organism.

Materials and Methods

Virtual screening and docking studies

JHCCL (ver1.2) was obtained from Johns Hopkins University, USA, and flexible docking studies of data sets were carried out using AutodockVina software. Otherwise mentioned, publicly available sources and databases were used for obtaining and processing of data. Three-dimensional structures of all the compounds were downloaded as SDF files and structures were refined with Open Babel 2.2.3 before docking studies.²⁶ The three-dimensional (3D) structure of β_2 AR was obtained from the Brookhaven Protein Data Bank (PDB).

Preparation of beta adrenergic receptor for docking

For docking, the 3D crystal structure of the β_2 AR receptor (PDB ID: 2RH1), resolved at 2.4 angstrom, was selected as a template and predocking approaches were exercised on the protein to increase the accuracy of the docking procedure. All the ligands, including the ones bound to the active site of β_2 AR, were removed from the crystal structure to facilitate the docking studies with molecules under investigation. The final steps of protein refinement, such as the addition of hydrogen atoms, computing charges, and merging nonpolar hydrogen atoms, were performed as mentioned.²⁷

Ligand preparation

The ligand data sets used were JHCCL and 23 known antagonists. Further processing and minimization were carried out with the help of Open Babel 2.2.3.

Parameter optimization for docking

AutoDockVina, the program used for docking, has been chosen over AutoDock 4 for its better accuracy and magnitude of processing speed.²⁸ AutoDockVina achieves around two orders of magnitude of processing speed compared with the AutoDock 4 software. This is vital when performing the screening of a large data set, and second, due to the superior binding model predicting ability in comparison with AutoDock 4. Apart from the speed and accuracy, it also works on parallelism by using multithreading on multicore machines.²⁹ The accuracy assessment and performance optimization were carried out before virtual screening of JHCCL. Crystal structure of the native ligand (carazolol) was isolated, minimized, and redocked in the binding pocket of β_2 AR. Comparisons were made between the conformations of the docked and crystal-bound ligand. Thereafter, efforts were made to find the best grid structure and coordinates. It was found that center_x = 31.724, center_y = -22.006, and center_z = -17.132 with the grid sizes of size_x = 30, size_y = 30, and size_z = 30 Å, respectively, were the best coordinates that covered the entire binding pocket of the target protein. Two aspects that strongly influenced the accuracy and performance of the docking performed by AutodockVina are num_modes, which represents the number of models to be evaluated, and exhaustiveness that increases the time for probabilistic search. To maximize the accuracy and performance, three different combinations of parameters were tried (10, 20, and 50 num_modes and 10, 20, and 50 exhaustiveness). Subsequently, 50 num_mode and 10 exhaustiveness

were opted as the final parameter because this combination elucidated the maximum accuracy with high speed. The ligand–protein complexes were minimized with 200 steps of steepest descent force field using Chimera and Discovery Studio.

Zebrafish husbandry and embryo collection

Wild-type (AB) and *Tg(cmyb:gfp)* zebrafish are kept at INMAS zebrafish facility on a 14-h light/10-h dark cycle at 28.5°C and all the experiments were carried out in accordance with the animal ethics guidelines of INMAS, Delhi, India (8GO/a/99/CPCSEA). Embryos from paired mating were collected, staged, and maintained in the embryo medium (E3 medium) at 28.5°C.³⁰ For visualization of internal structures, embryos were incubated with 0.003% 1-phenyl-2-thiourea (Sigma-Aldrich) to inhibit pigment formation.

Assessment of heart rate

Quantitative analysis of heart rate was performed following the stopwatch method.³¹ Briefly, todralazine (5 μ M) or metoprolol (5 μ M) was added to the medium containing embryos at 24 hour postfertilization (hpf). At 48 and 72 hpf, embryos were anesthetized using 0.04 mg/mL tricaine and the heart beat was counted for 1 min under the microscope (Dewinter) and results were expressed as average value of beats/min of three individual experiments; 0.04 mg/mL tricaine, used for inducing anesthesia, did not have any effect on the heart rate from 24 to 144 hpf staged embryos.

Chemically induced hemolytic anemia and quantification of erythrocytes

Hemolytic anemia was induced by incubating the dechorionated and staged embryos (33 hpf) in the E3 medium containing 0.5 μ g/mL of phenylhydrazine (PHZ) until 48 hpf, followed by thorough washing in the E3 medium. At 54 hpf, embryos were arrayed ($n = 10$ per treatment group) in a 48-well plate and small molecules were added at a concentration of 10 μ M and incubation was further continued till 96 hpf. o-Dianisidine (ODA) staining was used for quantifying the erythrocytes in caudal hematopoietic tissue (CHT).³² Briefly, at 96 hpf the embryos were washed and incubated in ODA staining buffer containing 0.6 mg/mL of o-dianisidine hydrochloride (Sigma Aldrich) in 10 mM sodium acetate (pH 5.2) and 4% ethanol. The activation of staining solution was achieved by adding hydrogen peroxide (20 μ L/mL; 30% stake) and kept at room temperature in the dark for 15 min, followed by extensive washing in phosphate-buffered saline (PBS) and fixing in 4% paraformaldehyde. Embryos positioned laterally were imaged (200 \times) using the brightfield microscope (Dewinter). For quantification, grayscale images were converted to binary images, and integral density of erythron pixels was calculated using Image J software (<http://imagej.nih.gov/ij/>, NIH).

*Chemically induced hemolytic anemia in *Tg(gata1a: dsRed)* embryos*

For visual assessment of chemically induced hemolytic anemia and its modulation by todralazine, *Tg(gata1a: dsRed)* embryos were treated as mentioned above, and imaging of CHT was done at 96 and 120 hpf (Zeiss Axioscope 40

fluorescent microscope; Carl Zeiss). Videos (Axiocam HR3; at least 15 s) of circulating erythrocytes within the caudal artery were recorded at 96 and 120 hpf.

Small-molecule treatment for identification of HSC expansion

Todralazine, identified from the preliminary screening was further tested for the HSC expanding potential. Wild-type age-matched embryos (24 hpf) were distributed in a 12-well plate and todralazine (5 μ M) or metoprolol (5 μ M) was added and incubated at 28.5°C until 36 hpf. Thereafter, the embryos were stored in RNAlater for RNA isolation. The expression of HSC markers (cMyb and runx1) was quantified using real-time polymerase chain reaction (qPCR).

RNA isolation, cDNA synthesis, and qPCR

Embryos stored in RNAlater (Qiagen) were cleaned, homogenized, and processed using an RNeasyPlus Micro kit (Qiagen) following the manufacturer's recommendations. Before RNA elution, each sample was digested with DNase to remove genomic DNA contamination using an RNase-free DNase set following the manufacturer's recommendations (Qiagen). RNA quality was checked in 2% formaldehyde agarose gel and RNA quantity and purity were determined by the Nano spectrophotometer (Implen). Two hundred fifty nanograms of total RNA was reverse transcribed using a Verso cDNA kit (Thermo Scientific) using oligodT primers. Relative levels of *runx1* or *cMyb* were quantified using qPCR. Primer pairs designed to cross intron–exon boundaries³³ were used and the expression levels were normalized to a reference gene (beta actin). Target and reference genes were amplified in separate wells in a 96-well plate using Quantifast SYBR green master mix (Qiagen) and using the Biorad FX98 machine (Biorad). qPCR conditions were at 94°C for 10 min, followed by 40 cycles at 95°C for 10 s, and at 60°C for 30 s. Relative fold change in gene expression was calculated by the $2^{-\Delta\Delta C_T}$ method.³⁴ In evaluating the nature of cells in the CHT region, wild-type zebrafish embryos, untreated or treated with todralazine (5 μ M) from 54 to 96 hpf, were anesthetized at 96 hpf. The tail (all tissue posterior to the opening of cloaca) was surgically separated and RNA was isolated and processed as mentioned above. The relative levels of erythroid-specific genes ($\beta e1$ and $\alpha e1$) were quantified using quantitative real time polymerase chain reaction.³⁵

Imaging of HSCs

For imaging of HSCs, todralazine (5 μ M) or metoprolol (5 μ M) was added to 24 hpf staged *Tg(cMyb:gfp)* embryos and incubation was continued till 36 hpf. After that, the embryos were anesthetized and HSCs were imaged (200 \times magnification) at the aorta-gonad-mesonephros (AGM) region using a fluorescence microscope (Ex 488 nm, Em 530 nm; Olympus). The number of HSCs residing in the AGM region was manually counted.

Radiation exposure and small-molecule treatment

Wild-type age-matched zebrafish embryos (24 hpf) were arrayed in a six-well plate and todralazine (5 μ M) or metoprolol (5 μ M) was added and after 30 min, embryos were exposed to 20 Gy gamma radiation using ⁶⁰Co source (Gamma

cell 5000, dose rate 1.02 kGy/h; AERB). Post irradiation, embryos were dechorionated and maintained at 28.5°C till 144 hpf and changes in gross morphology and survival were monitored every 24 h for 6 days. Photomicrography of embryos was done using an Olympus stereo zoom microscope (SZX16; Olympus) at 100× magnification. Further experiments with different concentrations of todralazine were done for identifying the optimal protective dose.

Quantification of pericardial edema and microphthalmia

Embryos positioned laterally were surveyed for eye size and the presence of pericardial edema (PE) and imaged using an Olympus microscope (SZX16; Olympus) at 100× magnification. Morphometric analysis of images was performed using Image J software and the area of eye and PE were measured in pixels and used for further analysis.

Quantification of reactive oxygen species in vivo

Reactive oxygen species (ROS) levels *in vivo* were detected in zebrafish embryos pretreated (–30 min) with todralazine (5 μM) and exposed to 20 Gy gamma radiation. Three hours post irradiation, the embryos were incubated with 5 μM dichlorofluorescein diacetate (DCFDA) for 20 min at 28.5°C in the dark,³⁶ followed by thorough washing in the E3 medium. Images were captured at 200× (under 488 nm excitation Leica, DMR) and the levels of ROS were quantified as fluorescent intensity (integral density) using Image J software.

Hydroxyl radical scavenging assay

Increasing concentrations of todralazine were added to PBS containing 2.8 mM of 2-deoxyribose (2-DR) in a final volume of 1 mL, and the mixture was exposed to 200 Gy gamma radiation. The extent of 2-DR degradation was measured by following the thiobarbituric acid (TBA) method.³⁷ To the mixture, 1 mL of TBA (1%, w/v in 0.05 M NaOH) and 1 mL of 2.8% trichloroacetic acid (TCA) were added and heated in a boiling water bath for 15 min. Thereafter, the samples were cooled and the absorbance of the chromogen was measured at 532 nm using a microplate reader (Spectramax M2^c; Molecular Devices). Results were shown as % inhibition and mannitol was used as a standard free radical scavenger.

In vivo detection of apoptosis

For quantification of apoptosis, todralazine (5 μM) was added to 24 hpf staged embryos and after 30 min exposed to gamma radiation (20 Gy). At 48 hpf, 2 μg/mL of acridine orange was added to the medium containing embryos and incubated in the dark for 30 min, which was followed by thorough washings in the E3 medium.³⁶ Notochord regions of the embryos were examined under 488 nm excitation and images were captured at 200× magnification (Leica, DMR). Fluorescence intensity (integral density) in three random areas of notochord per embryo was quantified using Image J software.

SubG1 population analysis

Embryos pretreated (–30 min) with todralazine (5 μM) and exposed to 20 Gy gamma radiation were processed for

quantification of apoptosis. Twenty-four hours after irradiation, embryos were dechorionated, washed, and disaggregated on ice in cold 0.9× PBS + 5% fetal bovine serum. The cell suspension was passed through a 40 μm filter to remove clumps and washed in the same buffer by centrifuging at 1000 rpm for 15 min at 4°C. The cell pellet was then gently suspended in 1 mL of propidium iodide solution (final concentration of 10 μg/mL). RNase was added to a final concentration of 2 μg/mL, incubated at room temperature for 30 min in the dark, and samples were analyzed using a flow cytometer (LSRII; Becton Dickinson). The cell cycle distribution and quantification of the subG1 population was done using flowing software (The Flowing Software, www.flowingsoftware.com, version 2.5.1, University of Turku, Finland).

Statistical analysis

Data are presented as mean ± SD of a minimum of three independent experiments and statistical significance was assessed by student's *t*-test, and a *p*-value < 0.05 was considered significant.

Results

The binding site of β₂AR and docking of JHCCL

The root mean square value calculated for assessing the accuracy and performance of the docking procedure was found to be 0.24 angstrom, suggesting the suitability for screening large data sets with both accuracy and speed. The conformation of the docked and crystal-bound ligand, carazolol, displayed a conserved binding pattern (Fig. 1a). The polar (Ser203, Asp113, Asn312) and hydrophobic interactions (Phe193, Trp109, Val114) were found to be the key intermolecular interactions in the binding pocket (Fig. 1a). Among them, Ser203, Val114, Asp113, and Asn132 are essential for antagonistic action. Docking of small molecules from JHCCL identified several small molecules with binding energy (BE) falling within the range reported for known antagonists (7.2 to 10.4 kcal/mol; Fig. 1b), and further visual inspection of properties related to similarity lead to the identification of 30 molecules (Table 1). The majority of the molecules showed classical carazolol-bound conformation (type 1) with key residues, Asp113 and Asn312, involved in the formation of hydrogen bonds (Fig. 1a, c). However, some of them have shown a binding conformation deviant (type 2) from the carazolol-binding mode (Fig. 1d). In this deviant mode, the stabilization of the ligands is achieved by hydrogen bonding with Ser203 and Tyr308 residues, while the latter interaction was found to be absent in the case of classical carazolol-binding conformation and uniquely contributes to the stability of the ligand in the deviant orientation. Val114 and Asn293, responsible for hydrophobic interactions, were also observed in the case of the type 2 binding (Fig. 1d).

Effect of todralazine on chemically induced hemolytic anemia and erythropoiesis in wild-type zebrafish embryos

Zebrafish embryos exposed to 0.5 μg/mL of PHZ from 33 to 48 hpf showed complete loss of circulating erythrocytes and anemia by 72 hpf. Removal of PHZ led to recovery of erythropoiesis by 120 hpf (data not presented). At 96 hpf,

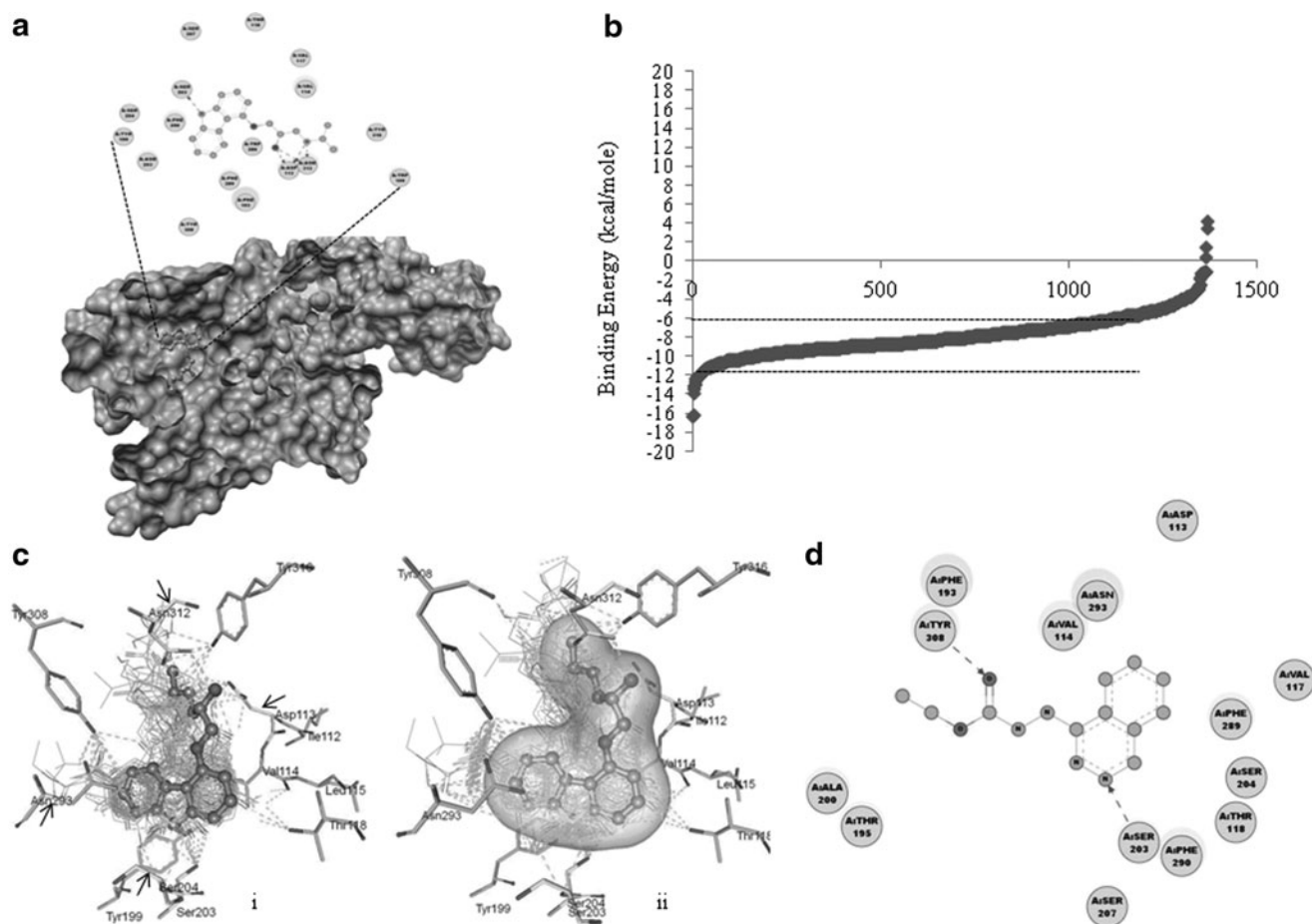


FIG. 1. (a) Space-filled side view of the β 2AR with bound carazolol. The proximal portion of the receptor has been removed for better viewing. The amino acid residues within 3 angstrom are shown as *circles*, and the *dashed arrow* represents hydrogen bonding between carazolol (*gray*) and amino acid residues (In view). (b) BE distribution for small molecules from the JHCCL. The region within the *dashed lines* indicates the BE range considered for further screening. The x-axis represents the number of compounds in the JHCCL. (c) (i) The binding pattern of 30 small molecules superimposed on the crystal-bound ligand (carazolol). The amino acid residues (Asp113, Ser203, Ser204, and Asn312), which are key for the binding are shown by *arrows*. (ii) The polar surface of the crystal-bound ligand and major contact in comparison with docked ligands. Hydrogen bonding is represented as *dashed lines*. (d) Two-dimensional view of crystal-bound todralazine (*gray*) showing intermolecular interactions. The amino acid residues within 3 angstrom are shown as *filled circles* and the hydrogen bonding between amino acid residues (Ser203 and Tyr308) and ligands are shown as *dashed arrows*. BE, binding energy; JHCCL, Johns Hopkins Clinical Compound Library.

PHZ-treated embryos showed lesser mature erythrocytes in the CHT (0.34-folds in comparison with an untreated control group; Fig. 2a, b). Initial screening of 30 small molecules, at a concentration of 10 μ M identified several molecules (66%; 20/30) accelerating the erythropoiesis and recovery from anemia (Table 1). Preliminary qualitative analysis of small molecules, which accelerated erythropoiesis, identified todralazine as the most efficient. Furthermore, dose optimization studies identified 5 μ M as the optimal concentration for todralazine. Treatment of wild-type zebrafish embryos with 5 μ M todralazine lead to an increase (2.3-folds) in the number of mature erythrocytes at CHT (Fig. 2a, b). Todralazine, at a concentration of 5 μ M, increased erythropoiesis in the CHT region (1.44-folds) in comparison with the anemic control (0.34-folds). Phenyl thiourea (0.003%) used to block the pigmentation in developing embryos did not affect the definitive hematopoiesis (Fig. 2a, left panel).

Effect of todralazine on chemically induced hemolytic anemia and erythropoiesis in $Tg(gata1a: dsRed)$ zebrafish embryos

As observed, in the case of wild-type zebrafish embryos, $Tg(gata1a: dsRed)$ zebrafish embryos also essentially recapitulated a similar response to PHZ-induced hemolytic anemia (Fig. 3i–vii). Untreated embryos have shown normal circulation of erythrocytes throughout the body, including caudal artery, intersegmental vessels, and CHT (shown by arrows), where imaging was done (Fig. 3i; Supplementary Video S1; Supplementary Data are available online at www.liebertpub.com/zeb). The CHT also showed several brightly strained erythroid progenitors (indicated by arrowheads; Fig. 3i). PHZ treatment led to induction of anemia by 72 hpf. Recovery was observed at both 96 and 120 hpf, as evident from the appearance of the erythrocytes and erythroid

TABLE 1. LIST OF 30 MOLECULES, WHICH HAVE BEEN TESTED FOR EFFECT ON RECOVERY FROM CHEMICALLY INDUCED HEMOLYTIC ANEMIA

Name of the Compound	Known pharmacological action	Binding energy (kcal/mol)	Phenotype
Norclozapine	Antipsychotic	-11	NS
Moricizine	Antiarrhythmic	-10.8	Positive
Mesoridazine	Antipsychotic	-10.5	Positive
Danthron	Laxative	-10.4	Positive
Chlorprothixene	Antipsychotic	-10.2	Positive
Rebamipide	Gastroprotective	-10.1	NS
Flavin mononucleotide	Co factor	-10	Positive
Thiethylperazine	Antiemetic., Antiemetic	-10	NS
Propantheline	Antispasmodic	-9.9	NS
Prochlorperazine	Antiemetic	-9.8	NS
4-(3,4-D)nM-1,2,3,4-T-1-amine	Corticotrophin-releasing factor receptor antagonist	-9.7	Positive
Fluphenazine	Antipsychotic	-9.7	Positive
Menadiol sodium phosphate hexahydrate	Vitamin (prothrombogenic)., Vitamin	-9.6	Positive
Imipramine	Antidepressant	-9.6	Positive
Pantethine	Antihyperlipidemic	-9.5	Positive
Acepromazine	Sedative	-9.5	Positive
Methantheline	Antispasmodic	-9.4	Positive
Desipramine	Antidepressant	-9.3	Positive
Triflupromazine	Antipsychotic	-9.3	NS
Clomipramine	Antidepressant	-9.3	NS
Thioridazine	Antipsychotic	-9.2	NS
Promethazine	Antihistaminic	-9.1	Positive
Triamterene	Antihypertensive	-9.1	Positive
Aminacrine	Antiseptic	-9.1	NS
Proflavine	Antiseptic	-9.1	Positive
Menadiol diacetate	Prothrombogenic vitamin	-9	Positive
Cephalosporin C zinc salt	Antibiotic	-8.4	NS
Todalazine hydrochloride	Antihypertensive	-8.4	Positive
Maprotiline	Antidepressant	-8.4	Positive
Harmaline	Vasorelaxant	-8.4	Positive

o-Dianisidine staining at the caudal hematopoietic tissue region was qualitatively compared between PHZ and PHZ + small-molecule-treated embryos. Positive: when the staining intensity is apparently more intense than the PHZ-treated group; NS: when staining is no different from the PHZ-treated group. Binding energy of different small molecules has been represented as (kcal/mol).

PHZ, phenylhydrazine.

progenitors at the CHT region (Fig. 3iv, v; Supplementary Video S2). At 96 hpf, there was no blood flow in the caudal artery and intersegmental vessels; however, at 120 hpf the PHZ-treated embryos showed recovery in terms of blood flow in the caudal artery and intersegmental vessels (indicated by arrows; Fig. 3iv, v). Todalazine treatment alone induced significant erythropoiesis at both 96 and 120 hpf as evident from intense fluorescence and number of erythroid progenitors (arrow head in Fig. 3ii, iii; Supplementary Video S3) in the CHT region. Embryos exposed to PHZ, followed by the treatment with todalazine, led to accelerated recovery from anemia at both 96 and 120 hpf as evident from the fluorescence circulating erythrocytes, brightly fluorescing progenitors in the caudal, intersegmental vessels, and the CHT region (Fig. 3vi, vii; Supplementary Video S4).

Effect of todalazine on erythroid progenitors in the CHT region: qPCR

RNA isolated from tails of untreated embryos (96 hpf) has demonstrated the presence of erythroid progenitors ($\alpha 1$ and $\beta 1$). However, tails from the embryos exposed to todalazine

(5 μ M) from 52 to 96 hpf showed increased levels of both $\alpha 1$ and $\beta 1$ RNA (1.34- and 1.21-folds, respectively) (Fig. 3b).

HSC expansion by todalazine: fluorescence microscopy

At 36 hpf, untreated *Tg(cmyb:gfp)* embryos at the AGM region showed resident HSCs (indicated by arrowheads; Fig. 4a, b). Todalazine, both at 5 or 10 μ M, increased the number of resident HSCs (~ 2.1 - and ~ 1.8 -folds, respectively) at the AGM region in comparison with the untreated control. Among the tested concentrations, 5 μ M was found to be optimal for HSC expansion (Fig. 4a, b). Metoprolol also increased the number of HSCs at the AGM region and both 5 μ M and 10 μ M (~ 1.6 - and ~ 1.75 -folds, respectively) were found to be equally effective (Fig. 4a, b).

HSC expansion by todalazine: qPCR

Quantification of HSC marker genes (*runx1* and *cMyb*) through qPCR following the Livak and Schmittgen $2^{-\Delta\Delta C_T}$ method, showed that treatment of embryos with 5 μ M todalazine

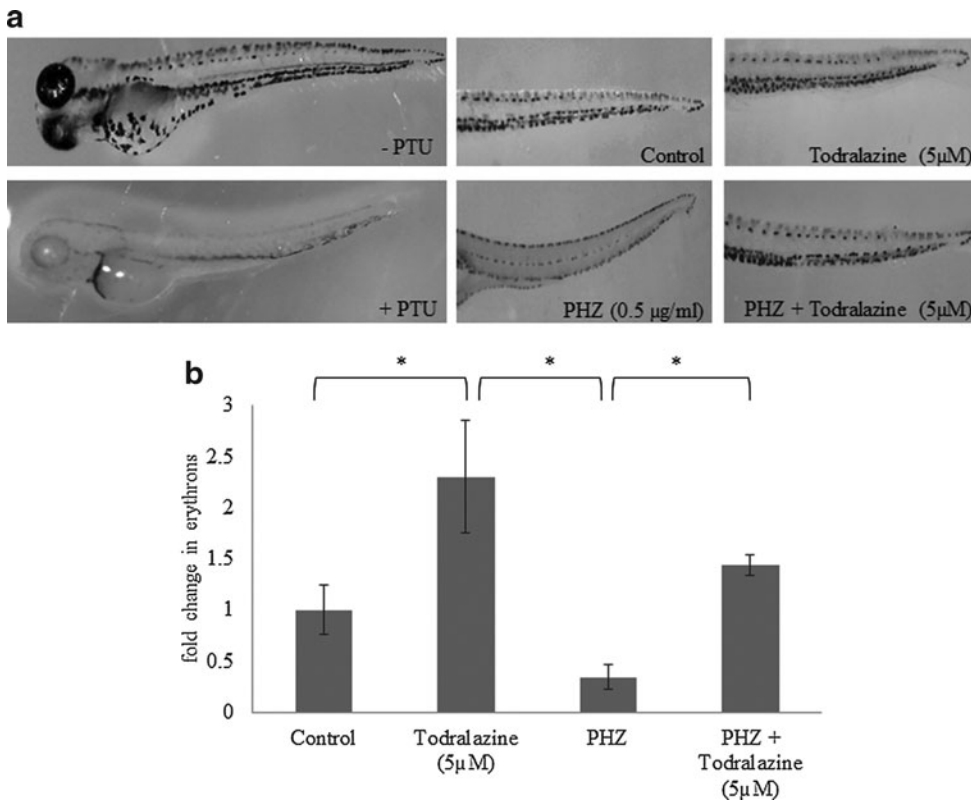


FIG. 2. Effect of todralazine on recovery from chemically induced hemolytic anemia in wild-type zebrafish embryos. **(a)** *Left panel:* representative images of o-dianisidine-stained embryos pretreated with 0.003% of phenyl thiourea; *Right panel:* representative images of different treatment groups are shown in the *right panel*. **(b)** PHZ and control embryos were treated with todralazine (5 μM) and monitored for formation of mature erythrocytes in caudal hematopoietic tissue (CHT) at 96 hpf by staining with o-dianisidine. Asterisk (*) indicates *p*-value < 0.05, when compared with control. hpf, hour postfertilization; PHZ, phenylhydrazine.

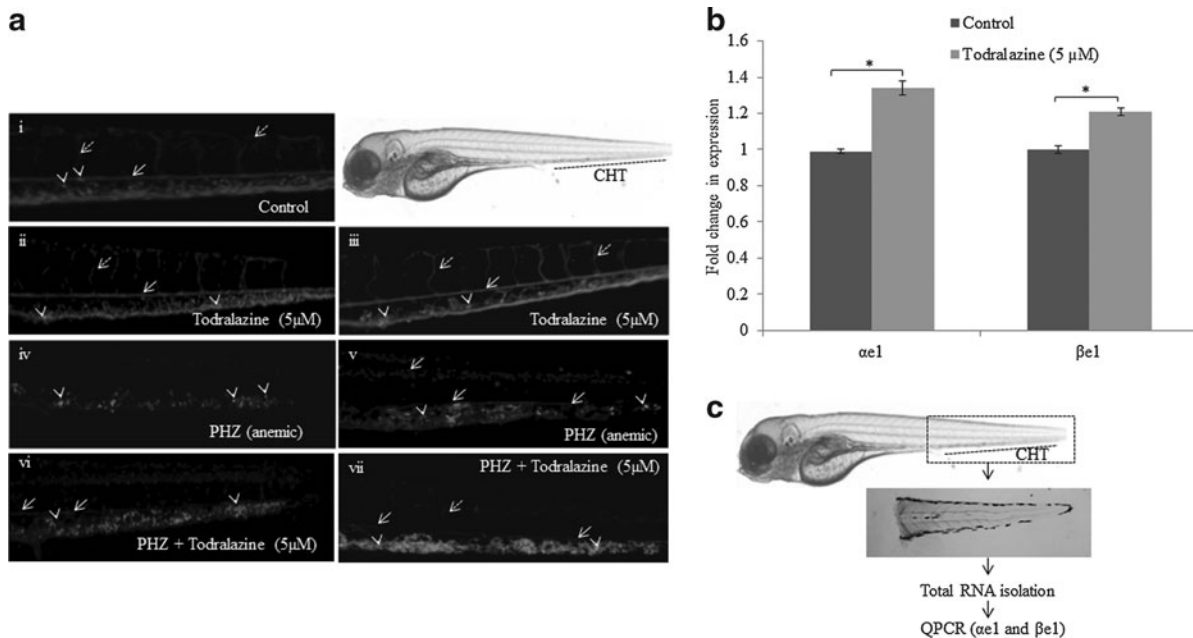


FIG. 3. Effect of todralazine on recovery from chemically induced hemolytic anemia in *Tg(gata1: dsRed)* zebrafish embryos. **(a)** Representative images of recovering embryos from PHZ-alone-treated embryos (**iv, v** at 96 and 120 hpf, respectively) or PHZ + todralazine treatments (**vi, vii** at 96 and 120 hpf, respectively). **(i)** Control embryos at 96 hpf and **(ii, iii)** are todralazine-alone-treated embryos at 96 and 120 hpf, respectively. *Solid and dashed arrows* points to intersegmental vessel (Se) and caudal artery, respectively. *Arrowhead* points to the brightly fluorescing erythroid progenitor population within the CHT region. **(b)** Quantitative real-time PCR analysis of expression of erythroid progenitor markers (*αe1* and *βe1*) in wild-type zebrafish embryos. **(c)** A schematic representation of the experimental protocol of the gene expression analysis in the surgically separated tails of untreated or todralazine-treated wild-type zebrafish embryos. Asterisk (*) indicates *p*-value < 0.05, when compared with control. CHT, caudal hematopoietic tissue; PCR, polymerase chain reaction.

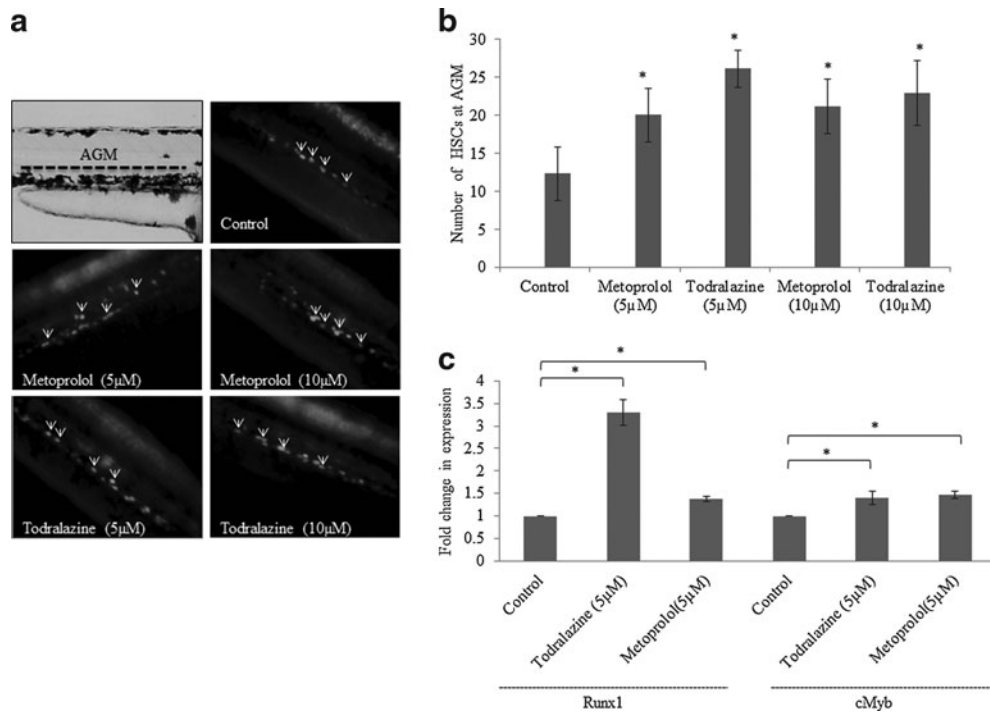


FIG. 4. (a) Representative images of HSCs (pointed by arrowhead) at the AGM region in todralazine (5 or 10 μM) or metoprolol (5 or 10 μM)-treated Tg(cmyb:GFP) zebrafish embryos. (b) Histogram of number of HSCs at the AGM region in treated and untreated embryos. (c) Quantitative real-time PCR analysis of expression of HSC marker genes in zebrafish embryos. Asterisk (*) indicates p -value < 0.05 , when compared with control. AGM, aorta-gonad-mesonephros; HSCs, hematopoietic stem cells.

from 24 to 36 hpf led to increased expression of *runx1* (3.3-folds) and *cMyb* (1.4-folds) in comparison with an untreated control group (Fig. 4c). Similarly, metoprolol (5 μM) also increased the expression of both *runx1* (1.38-folds) and *cmyb* (1.46-folds) in comparison with untreated controls (Fig. 4c).

Effect of todralazine on heart rate in wild-type zebrafish embryos

To understand the functional consequence of the β_2 blockade, the effect on heart rate was assessed. Metoprolol, a known beta blocker, slowed the heart rate in a dose-dependent manner, assessed after 24 and 48 h of treatment. Maximal reduction (27%) was noted after 24 h at the highest concentration tried in this field (100 μM ; Fig. 5). By 48 h, metoprolol-treated embryos displayed recovery, and at 100 μM concentration the heart rate was found to be 12%. Todralazine, though to a lesser extent in comparison with metoprolol, also slowed the heart rate in a dose-dependent manner and maximally (12%) at 100 μM . The lower concentrations (5, 10, and 20 μM)-induced reduction in heart rate was recovered by 48 h of todralazine treatment. However, higher concentration-mediated (50, 100 μM) reduction was found to be persistent even after 48 h of treatment. At 100 μM , after 48 h, the heart rate in todralazine-treated embryos was 12% (Fig. 5).

Modulation of radiation-induced damage and lethality by todralazine

Untreated wild-type embryos displayed a continuous increase in the eye size (100% embryos exhibited this

phenotype) till 3 day post fertilization (dpf) with no further significant increase for the rest of the experimental duration (Fig. 6a, b). The eye size reduction and PE, end points used to evaluate the radioprotection efficacy of the molecules, are associated with poor development of the embryos and they represent a general response to toxicants. Exposure to 20 Gy

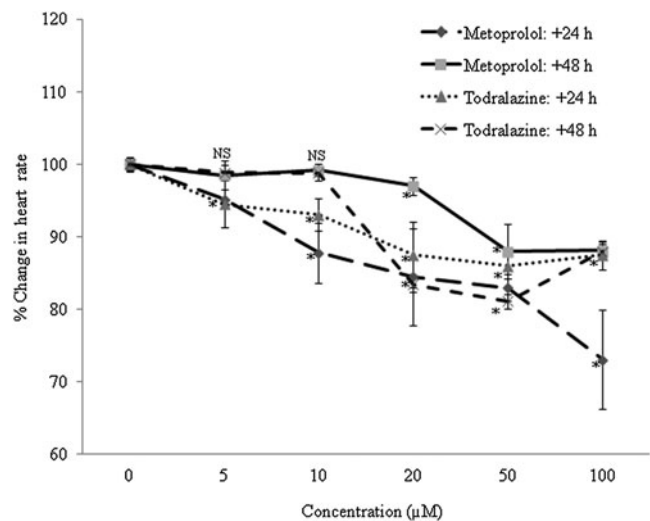


FIG. 5. Effect of varied concentrations of todralazine or metoprolol on heart rate at 24 and 48 h post-treatment in wild-type zebrafish embryos. Asterisk (*) indicates p -value < 0.05 , when compared with control. NS, not significant, when comparison was made between control and treated groups.

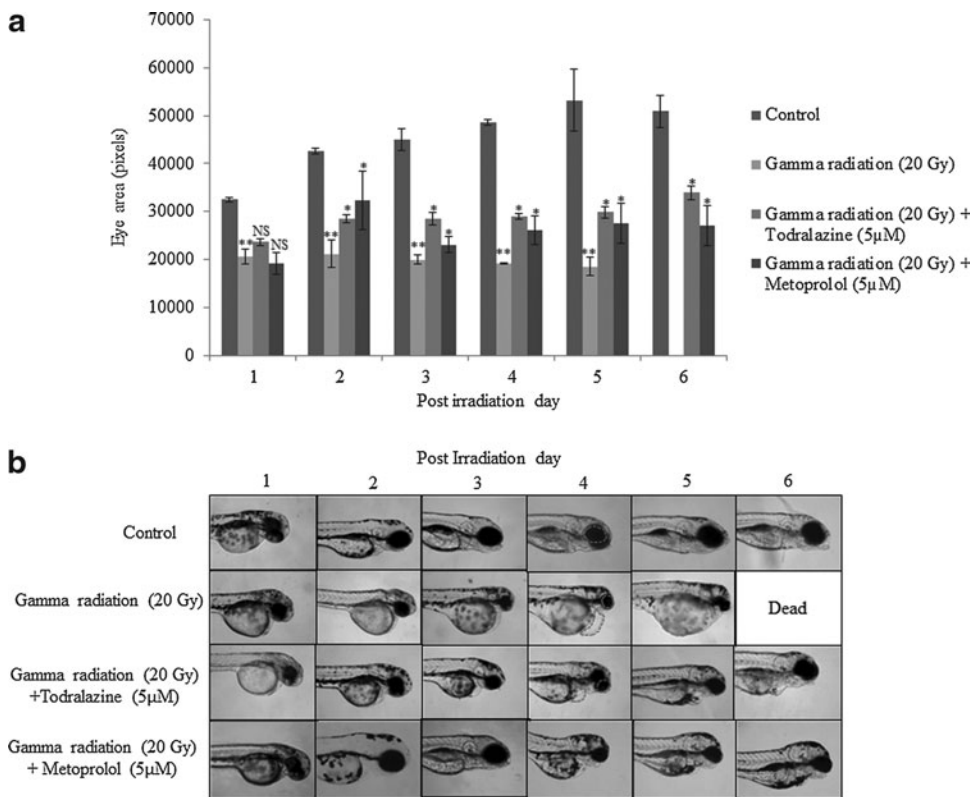


FIG. 6. Effect of todralazine ($5 \mu\text{M}$) or metoprolol ($5 \mu\text{M}$) on radiation-induced effects on eye size. **(a)** Embryos were exposed to 20 Gy gamma radiation in the presence or absence of $5 \mu\text{M}$ todralazine treatment and the eye size was observed till 6th postirradiation day. **(b)** Representative images of different treatment groups are shown for different postirradiation days. The eye and pericardial edema evident within different treatment groups is highlighted with the dotted line. Asterisk (*) indicates p -value < 0.05 , when compared with radiation alone. NS, not significant, when compared with the radiation-alone group. (**) indicates p -value < 0.05 , when compared with control group.

led to a significant slowing down of eye development and eye size ($> 85\%$ embryos) in comparison with untreated controls (Fig. 6a, b). The decline in eye size was evident till the embryos were dead. Todralazine ($5 \mu\text{M}$), added 30 min before irradiation, protected embryos from radiation-induced decline in eye size and the protective effect ($> 80\%$ embryos) was pronounced from 3 dpf till the end of the experiment. Similarly, metoprolol ($5 \mu\text{M}$), when added 30 min before irradiation, showed a significant protection ($> 85\%$ embryos) trend similar to that of todralazine (Fig. 6a, b). The 20 Gy gamma radiation exposure significantly increased the area of PE ($> 85\%$ embryos) in comparison with untreated control groups and a continuous increase was observed till the embryos were dead (Figs. 6b and 7a). There was a steep increase in the edema size on day 4 after irradiation. Todralazine, added before irradiation, persistently reduced the radiation-induced PE till the end of the experiment ($> 85\%$ embryos). Metoprolol, at a concentration of $5 \mu\text{M}$, manifested a protection trend similar to that of todralazine during the course of the experiment ($> 85\%$ embryos; Figs. 6b and 7a). Untreated wild-type embryos showed normal development without gross deformities. However, exposure to 20 Gy gamma radiation induced severe gross deformities, including reduction in eye size, PE, microcephaly, cup-shaped spine, yellow pigmentation, and stunted growth ($> 90\%$ embryos). These deformities were found to increase in severity with time. In the present study, all the embryos were found to be dead by the sixth postirradiation day (Fig. 7b). Todralazine ($5 \mu\text{M}$) or metoprolol ($5 \mu\text{M}$) when added 30 min before irradiation protected embryos from lethality and rendered $> 80\%$ survival advantage (Fig. 7b). Apart from the survival advantages, the embryos showed reduced deformities ($> 85\%$ embryos) (Fig. 6b).

Hydroxyl radical scavenging by todralazine

Exposure of 2-DR solution to a 200 Gy gamma radiation resulted in deoxyribose degradation and formation of TBA-reactive substances, which in the presence of TCA interacted with TBA and formed pink chromogen. Todralazine, in a dose-dependent manner, inhibited hydroxyl radical-mediated 2-DR degradation and chromogen formation (Fig. 8a). In this study, 21% inhibition was observed at the lowest concentration tried ($5 \mu\text{M}$) and the protective effect was found to be dose dependent. Maximum inhibition (45%) was observed at the highest concentration tried in this study (1 mM). Mannitol, a standard free radical scavenger, did not show hydroxyl radical scavenging at lower concentrations (below 0.5 mM) (Fig. 8a). However, at concentrations higher than 0.5 mM, it displayed significant, though less than todralazine, hydroxyl radical scavenging potential.

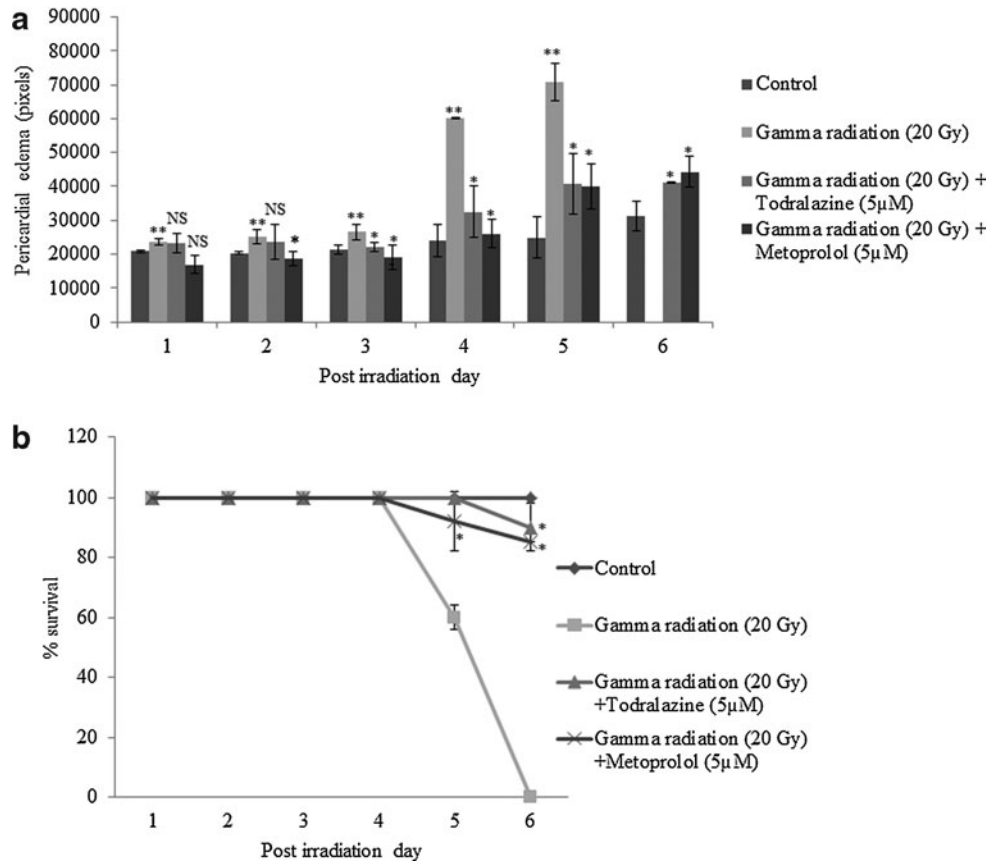
ROS scavenging in vivo: DCFDA assay

Gamma radiation (20 Gy) significantly increased the generation of reactive free radicals in zebrafish embryos, as evident from increased DCF fluorescence (1.85-fold increase when compared with the untreated control). However, todralazine ($5 \mu\text{M}$), when added before irradiation effectively scavenged radiation-generated free radicals as seen from the decrease in DCF fluorescence (1.56-folds) (Fig. 8b, c).

Todralazine limits radiation-induced apoptosis

A dose of 20 Gy gamma radiation increased the quantum of cells undergoing apoptosis (acridine orange-positive cells) in the developing zebrafish embryos ($163,915 \pm 17,450$ arbitrary fluorescence units [AFU]) when compared with the

FIG. 7. Effect of todralazine (5 μ M) or metoprolol (5 μ M) on radiation-induced pericardial edema. **(a)** Embryos were exposed to 20 Gy gamma radiation in the presence or absence of 5 μ M todralazine or metoprolol and the formation of pericardial edema was observed till 6th postirradiation day. **(b)** Effect of todralazine on radiation-induced mortality in zebrafish embryos. Twenty-four hpf embryos were exposed to 20 Gy gamma radiation in the presence or absence of 5 μ M todralazine or metoprolol and survival (with beating heart) was monitored till 6th postirradiation day. Asterisk (*) indicates p -value < 0.05, when compared with radiation alone. NS, not significant, when compared with the radiation-alone group. (**) indicates p -value < 0.05, when compared with control group.



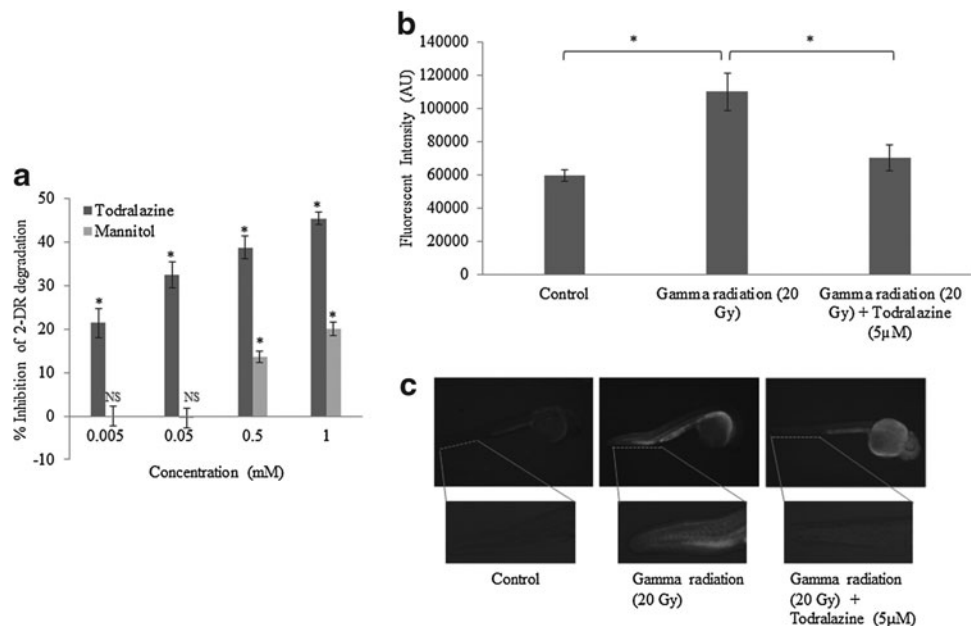
untreated control ($94,426 \pm 29,415$ AFU). Embryos treated with 5 μ M todralazine limited radiation-induced apoptotic induction ($101,101 \pm 26,497$ AFU) (Fig. 9a, b). Flow cytometric analysis of the cell suspension prepared from developing whole embryos after 24 h of sham or gamma radiation (20 Gy) exposure, exhibited a subG₀ population of 1.48% and 10.6%, respectively. Irradiated embryos pretreated with

todralazine showed decrease in apoptotic population (subG₀ population) after 24 h (Fig. 9c).

Discussion

The autonomic nervous system regulates several cellular and molecular signaling cascades in normal and pathological

FIG. 8. **(a)** Radiation-induced OH radical scavenging potential of todralazine or mannitol at varying concentrations; inhibition of chromogen was calculated with respect to control, which was considered as zero inhibition. **(b)** Effect of todralazine on radiation-induced reactive oxygen species measured in the notochord region of the embryos, by DCFDA staining, 3 h after radiation exposure. The integral density in the notochord region of different treatment groups was calculated using image J software. **(c)** Representative images showing DCF fluorescence in the whole embryos. Asterisk (*) indicates p -value < 0.05, when compared with radiation alone. DCFDA, dichlorofluorescein diacetate. NS, not significant, when compared with radiation alone.



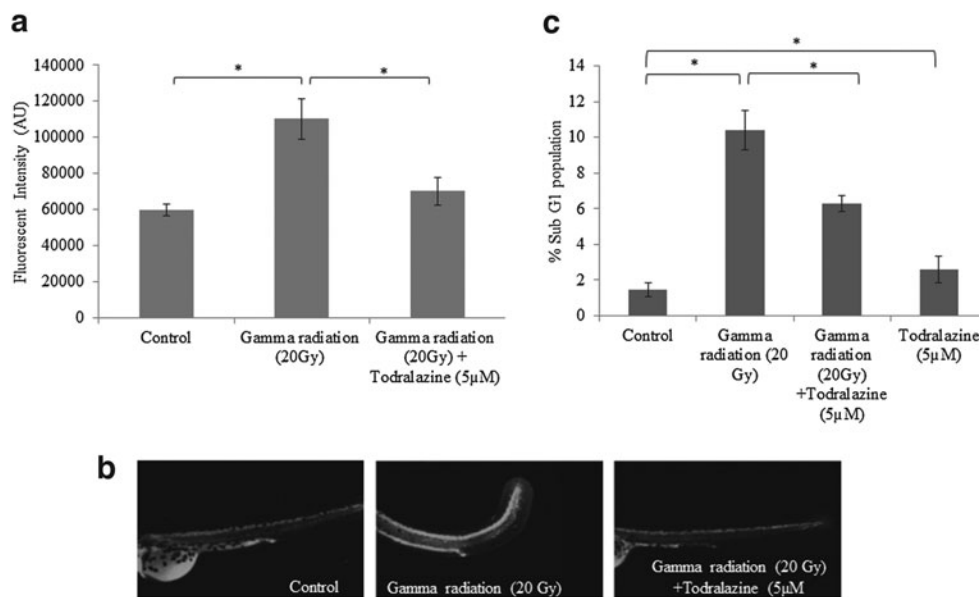


FIG. 9. (a) Effect of todralazine on radiation-induced apoptosis, measured in the notochord region or in whole embryos, 24 h after irradiation, by the acridine orange method. The integral density in the notochord region of different treatment groups was calculated using image J software. (b) Representative images showing acridine orange fluorescence in the notochord of the embryos. (c) Effect of todralazine on radiation-induced apoptosis measured in cell suspension prepared from the whole embryo 24 h after irradiation using flow cytometry and subG1 population was considered as apoptotic cells. Asterisk (*) indicates p -value < 0.05 , when comparison is done between indicated groups.

conditions, including hematopoiesis, cancer, and stress response.³⁸ Over the past six decades, a number of β_2 AR ligands have been identified on the basis of ligand analogue. In fact, G protein-coupled receptors are among the most frequent targets for a number of drugs and several of them target β_2 AR.³⁹ Trauma-induced catecholamine surge suppresses the bone marrow HSPC growth and increases the mobilization of HSC to the site of the trauma.⁴⁰ β_2 AR receptor antagonists block the trauma-induced mobilization of HSCs, thereby making the β_2 AR receptor modulation a potential strategy for HSC expansion.^{40,41} The narrow deep cleft majorly hidden from the solvent makes the catecholamine (epinephrine)-binding site in β_2 AR a potential site for molecular docking.^{42,43} In fact, this narrow deep cleft has been exploited for screening of compound libraries for identification of novel β_2 AR ligands.⁴⁴ In this study, docking of JHCLL into the carazolol-binding site identified several potential antagonists. The docking program used in the present study reliably performed the docking, as evident from the similar conformation and intermolecular interactions of the docked carazolol to that reported for crystal-bound carazolol.⁴⁴ The screening identified a number of small molecules with potential for being β_2 AR ligands. As both agonists and antagonists bind at the same site, reliable identification of a particular type of ligand on the basis of BE yields false-positive hits. Therefore, a visual inspection of the primary hits recognized on the basis of BE was evaluated. The cutoff BE was estimated from the BE of known antagonists (-7.2 to -10.5 kcal/mol). The key intermolecular interactions (Ser203, Val114, Asp113, and Asn132), critical for antagonistic action, were considered for prioritizing the hits. Recently, we have observed that known antagonists (23) adopt either of two different conformations in the carazolol-binding pocket of β_2 AR. The first one is the classical carazolol

orientation and the second type adopts distinct bridge-type conformation (under communication). This finding opened opportunities to screen the molecules based on novel orientation. Therefore, the final set of prioritized molecules is the result of the combination of BE, antagonist-binding interactions, and the novel binding orientation. These hits were evaluated for possible HSC expanding potential using erythropoiesis in anemic zebrafish embryos as a functional test.

PHZ induces reversible hemolytic anemia in a variety of species, and induction of oxidative stress in erythrocytes is one of the important events in the PHZ-induced hemolytic anemia cascade.⁴⁵ In the bone marrow, HSCs differentiate to common myeloid and lymphoid progenitors and the former further give rise to erythroid and granulocyte/monocyte progenitors, while common lymphoid progenitors develop immune components.⁴⁶ In the case of hemolytic anemia and other stresses, loss of mature erythrocytes induces feedback signaling leading to increased formation of erythrocytes.^{47,48} PHZ-induced hemolytic anemia has been a valuable approach for assessing the HSPC expanding potential of different agents.⁴⁹ PHZ-induced hemolytic anemia is reversible in nature and the anemic condition persists as long as the PHZ is in the medium. Removal of PHZ leads to the recovery phase and normal levels of erythrocytes are achieved by 5 dpf in zebrafish embryos.⁴⁹ Preliminary studies from our laboratory suggested 96 hpf as the earliest time point where the differences between the normal and drug-induced recovery could reliably be differentiated on the basis of ODA staining. Hence, 96 hpf was chosen as the time point for drug-induced recovery studies. Todralazine, an antihypertensive drug from the hydrazine-ophthalazine group, at a concentration of $5 \mu\text{M}$, significantly accelerated erythropoiesis. Among the 30 small molecules identified through virtual screening, several molecules showed better BE. However, preliminary

qualitative screening for enhancing erythropoiesis lead to identification of todralazine as the most potent one. Out of the 30 molecules put into screening, a few molecules did not exert any influence at the concentration (10 μ M) used for screening (Table 1). However, it does not rule out the possibility of these molecules being potential, as the screening concentration (10 μ M) may not be optimal for these compounds. Further studies with a range of concentrations are warranted to identify the optimal concentrations for these compounds. Several studies have clearly suggested that PHZ induces hemolytic anemia through generation of free radicals, peroxidation of lipids, and apoptosis.⁴⁵ Antioxidant treatment is known to ameliorate PHZ-induced hematotoxicity. However, in the present study, PHZ treatment was given from 33 to 48 hpf, followed by repeated changes in E3 to remove traces of PHZ before todralazine addition. Therefore, free radical scavenging and antiapoptotic action as a mechanism for rescuing zebrafish from PHZ-induced hemolytic anemia can be ruled out. To visually assess the influence of todralazine on recovery from hemolytic anemia, *Tg(gata1a:dsRed)* zebrafish embryos were used. GATA1, an erythroid-specific transcription factor, marks erythroid lineage⁵⁰ and regulates vital developmental processes in vertebrates, including hematopoiesis.⁵⁰ The GATA1 reporter zebrafish has been well characterized and used for understanding the dynamics of erythroid progenitors in live embryos.^{49,50} In the present study, *Tg(gata1a:dsRed)* zebrafish embryos essentially recapitulated the effects of PHZ and todralazine observed in wild-type embryos. Long *et al.*, using the *Tg(gata:gfp)* reported the presence of two distinct populations based on fluorescent intensity, one being larger and brighter, while the other being smaller and less bright.⁵⁰ Furthermore, transplantation studies with the sorted population suggested that a larger and brighter population harbors long-term repopulating potential and represents erythroid progenitors. In view of these studies, we tried to assess the nature of cells present in the CHT region in different experimental groups. Fluorescence microscopy clearly showed brightly fluorescent and less brightly fluorescent populations. At both 96 and 120 hpf, the CHT region harbored these brightly fluorescent erythroid progenitor populations, which seem to be responsible for erythropoiesis (Fig. 3a). To further ascertain the nature and presence of erythroid progenitors in the CHT region, tails from untreated and todralazine-treated embryos were surgically removed at 96 hpf and erythroid-specific gene expression (α e1 and β e1) was analyzed using qPCR. A similar approach, involving surgically separating the trunk from the tail to study the role of different hemogenic sites (trunk and tail) in definite erythropoiesis has been done by several investigators.^{51,52} The results clearly suggest the presence of erythroid-specific progenitors responsible for definitive erythropoiesis at CHT (Fig. 3b). These results are in corroboration with earlier studies, which report that in wild-type developing embryos, at 96 hpf, both the trunk and CHT region contribute toward the definitive erythropoiesis.^{51,52}

Erythropoiesis is one of the committed downstream functions of HSCs and several small molecules are known to influence the HSCs and their expansion.^{11,13} Therefore, it was interesting to assess the influence of todralazine on HSCs. To assess the effect of todralazine on HSC expansion, imaging of HSCs at the AGM region at 36 hpf was done in *Tg(cmyb:gfp)* embryos. *cMyb* is a well-known marker for definitive HSCs,

and it is well known that definitive HSC production ensues in the AGM region along the ventral wall of the dorsal aorta subsequently colonizing CHT, thymus, and eventually the kidney.⁵³ Several investigators have used the AGM region to visually identify HSC expanding potential of the small molecule.^{10,13} Imaging in the AGM region at 36 hpf, has clearly suggested that todralazine (5 or 10 μ M) increased (\sim 2- and 1.8-folds, respectively); the number of HSCs indicating its HSC expanding potential (Fig. 4a, b). Similarly metoprolol, a known β blocker and antihypertensive drug, also increased the number of HSCs (\sim 1.7-folds) (Fig. 4a, b).

To further prove the HSC expanding potential of β_2 blockers, expression of HSC markers (*runx1* and *cMyb*) was assessed in case of todralazine or metoprolol-treated wild-type zebrafish embryos (Fig. 4c). Todralazine treatment from 24 to 36 hpf led to increased expression of both *runx1* and *cMyb*, indicating expanded HSC pool. In the present study, the drugs were added at 24 hpf because β_2 blockers are known to expand the HSC pool more effectively when added after commencing of blood flow.¹³ In the case of zebrafish, the blood flow begins at around 24 hpf. Many blood flow altering agents with beta adrenergic receptor antagonist potential increase the proliferation of HSCs,¹³ further supporting the use of β_2 AR as a target for identification of novel HSC expanding agents. As the aim of the present work was to identify agents that can render protection against lethal doses of gamma radiation, the radioprotective effect of todralazine was tested in developing zebrafish embryos. Among the early developmental stages, the mid-blastula transition stage is the most radiosensitive stage suitable for screening agents for radiation protection.⁵⁴ However, in this study, 24 hpf staged embryos were used for radioprotection experiments, as a sizeable fraction of embryos either die or do not develop normally in the first 24 hpf. Those embryos, which survive the first 24 h develop normally and reach adulthood. In the present study, 144 hpf was used as the time limit for assessing mortality and organ damage because the first 6 days of the developing embryos are independent of external feeding, thereby reducing the variability in terms of differences in feeding ability after irradiation. In fact, a similar screening schedule was used by several investigators for identifying radioprotectors.⁵⁴⁻⁵⁶ Todralazine, at a concentration of 5 μ M, added 30 min before the 20 Gy gamma radiation exposure, significantly protected the embryos, both from lethality and radiation-induced organ toxicity, assessed as PE and eye size (Figs. 8 and 9). To further understand a possible correlation between β_2 blockade, HSC expansion, and radioprotection, metoprolol, a known beta blocker, was tested for possible radiation protection. Metoprolol, showed both HSC expansion potential and the ability to protect zebrafish embryos from radiation-mediated lethality. However, further studies are required to prove a direct relationship between β_2 blockade, HSC expansion, and radioprotection. Several studies suggested that beta blockers, including metoprolol, exert adrenoceptor-independent effects, including free radical scavenging and antioxidant action.⁵⁷ It can be expected that radiation protection by metoprolol could at least be partially attributed to its antioxidant actions. Radiation-mediated damages involve generation of free radicals, macromolecule degradation, and oxidative stress and in relevance to these, free radical scavenging potential has evolved as one of the important radioprotective mechanisms. In fact,

todralazine has already been reported to exert antimutagenic action.⁵⁸ It was interesting to understand the contributory role of free radical scavenging in its overall radioprotective action. 2-DR assay is a reliable test to assess the hydroxyl radical scavenging potential of molecules in a cell-free system.³⁷ Todralazine inhibited hydroxyl radical-mediated degradation of 2-DR, suggesting its radical scavenging potential (Fig. 8a). However, one of the major problems with antioxidants is that they often do not faithfully recapitulate the same potential *in vivo*, hence, the ROS scavenging potential of todralazine was tested *in vivo*. As shown, through the 2-DR degradation assay (*in vitro*) todralazine at the radioprotective concentration (5 μ M) scavenged ROS *in vivo* as well (DCFDA assay). These results are in corroboration with an earlier study by Gasiorowski, which reports the antimutagenic potential of todralazine.⁵⁸ To confirm its ROS scavenging potential *in vivo*, apoptosis, a downstream effect of free radical-mediated oxidative damage was assessed in different treatment groups using the acridine orange assay. Apoptosis was observed throughout the developing embryos. However, for quantifying apoptosis, the notochord of the embryos was considered due to the high radiosensitivity of developing notochord.⁵⁹ Todralazine protected the embryos from radiation-induced apoptosis, further proving its free radical scavenging and antioxidant action. Quantification of apoptotic cells, identified as the subG1 population, using the flow cytometry technique further supported the capacity of todralazine to block radiation-induced apoptosis. Overall, the results suggested that todralazine possesses the HSC expanding and antioxidant potential, which might be contributing toward its radioprotective action. Since, in the present study, todralazine was added before irradiation, the free radical scavenging and antioxidant action might be the major radioprotective mechanism with HSC expanding potential as the contributory mechanism. Studies on the radiomitigative potential of todralazine are warranted to establish the role of HSC expanding potential toward its radioprotective action.

Molecular docking studies have indicated possible β_2 blockade by todralazine, and to further establish the same, the effect on heart rate was assessed. Beta blockers are known for their antihypertensive action and an important downstream functional effect of the β_2 blockade is the slowing down of heart rate and reduced blood pressure.⁶⁰ Several beta blockers reduce heart rate in a variety of animal models, including zebrafish.⁶¹ Todralazine, in a dose-dependent manner, reduced heart rate in developing zebrafish embryos (Fig. 5), supporting the possible β_2 blockade action. However, direct receptor and ligand-binding studies are warranted for unequivocally proving the interaction. Nevertheless, it is worthwhile to mention the fact that the β_2 AR-binding potential of todralazine can also be anticipated from the fact that todralazine is an antihypertensive drug and β_2 AR could be its target in view of the notion that molecules sharing similar functions are likely to share targets as well.⁶² However, it is interesting to understand adrenoreceptor-independent mechanisms, such as modulation of epigenetic status of the cell, as many epigenetic-modulating agents (HAT inhibitors) effectively modulate hematopoiesis.^{12,63,64} In fact, todralazine has been reported to inhibit histone acetylation.⁶⁴ The present study reports HSC expansion and radiation protection by todralazine, an antihypertensive drug in clinical use. As the radiation-induced hematopoietic syndrome is the

predominant cause of mortality, its utility as an HSC expanding agent in postirradiation scenarios holds significant implications. However, validation of HSC expansion and radioprotective potential in murine models and higher mammals, including nonhuman primates, is key for translating todralazine for possible applications in the management of radiation overexposed victims.

Acknowledgments

The authors thank Dr. R.P. Tripathi, Director, INMAS, for constant support and encouragement; DRDO for funding; Dr. Leonard I. Zon, Harvard University, USA, for *Tg(cmyb:gfp)*; Dr. Sridhar Sivasubbu, Institute of Genomics and Integrative Biology, Delhi, India, for experiments related to *Tg(gata1a:dsRed)*; Dr. Sheng-Ping Hwang, Taiwan Zebrafish Core Facility, Taiwan, for the work related to *Tg(cmyb:gfp)*; and Johns Hopkins University, USA, for JHCCL. Manali Dimri gratefully acknowledges the DRDO fellowship.

Disclosure Statement

The authors declare no competing financial interests.

References

1. Prem Kumar I, Gupta D, Bhatt AN, Dwarakanath BS. Models for the development of radiation countermeasures. *Def Sci J* 2011;61:1–8.
2. Dörr H, Meineke V. Acute radiation syndrome caused by accidental radiation exposure—therapeutic principles. *BMC Med* 2011;9:126.
3. Xiao M, Whitna MH. Pharmacological countermeasures for the acute radiation syndrome. *Mol Pharmacol* 2009;2:122–133.
4. Pogożelski WK, Xapsos MA, Blakely WF. Quantitative assessment of the contribution of clustered damage to DNA double-strand breaks induced by 60Co gamma rays and fission neutrons. *Radiat Res* 1999;151:442–448.
5. Greenberger JS, Clump D, Kagan V, Bayir H, Lazo JS, Wipf P, *et al.* Strategies for discovery of small molecule radiation protectors and radiation mitigators. *Front Oncol* 2012;1:59.
6. Weiss JF, Landauer MR. Radioprotection by antioxidants. *Ann N Y Acad Sci* 2000;899:44–60.
7. Lorenz E, Uphoff D, Reid TR, Shelton E. Modification of irradiation injury in mice and guinea pigs by bone marrow injections. *J Nat Cancer Inst* 1951;12:197–201.
8. Ding S, Schultz PG. A role of chemistry in stem cell biology. *Nat Biotechnol* 2004;22:833–840.
9. Gosselin J, Sii-Felice K, Leboulch P, Tronik-Le Roux D: Searching for the key to expand hematopoietic stem cells. In: *Advances in Hematopoietic Stem Cell Research*. Pelayo R (ed.), ISBN: 978-953-307-930-1, InTech, Croatia. Available from: www.intechopen.com/books/advances-in-hematopoietic-stem-cell-research/searching-for-the-key-to-expand-hematopoietic-stem-cells
10. North TE, Goessling W, Walkley CR, Lengerke C, Kopani KR, *et al.* Prostaglandin E2 regulates vertebrate hematopoietic stem cell homeostasis. *Nature* 2007;447:1007–1011.
11. Boitano AE, Jian Wang J, *et al.* Aryl hydrocarbon receptor antagonists promote the expansion of human hematopoietic stem cells. *Science* 2010;39:1345–1348.
12. Nishino T, Wang C, Mochizuki-Kashio M, Osawa M, Nakauchi H, Iwama A. Ex vivo expansion of human he-

- matopoietic stem cells by garcinol, a potent inhibitor of histone acetyl transferase. *PLoS One* 2011;6:e24298.
13. North TE, Goessling W, Peeters M, Li P, Ceol C, Lord AM, *et al.* Hematopoietic stem cell development is dependent on blood flow. *Cell* 2009;137:736–748.
 14. Ashburn TT, Thor KB. Drug repositioning: identifying and developing new uses for existing drugs. *Nat Rev Drug Discov* 2004;3:673–683.
 15. Kim K, Pollard JM, Norris AJ, McDonald JT, Sun Y, Micewicz E, *et al.* High throughput screening identifies two classes of antibiotics as radioprotectors: tetracyclins and fluoroquinolones. *Clin Cancer Res* 2009;15:7238–7245.
 16. Huang HT, Kathrein KL, Barton A, Gitlin Z, Huang YH, Ward TP, *et al.* A network of epigenetic regulators guides developmental haematopoiesis *in vivo*. *Nat Cell Biol* 2013;15:1516–1525.
 17. Williams C, Kim S, NI TT, Mitchell L, Ro H, Penn JS, *et al.* Hedgehog signaling induces arterial endothelial cell formation by repressing venous cell fate. *Dev Biol* 2010;341:196–204.
 18. Ablain J, Zon LI. Of fish and men: using zebrafish to fight human diseases. *Trends Cell Biol* 2013;23:584–586.
 19. Das BC, McCormick L, Thapa P, Karki R, Evans T. Use of zebrafish in chemical biology and drug discovery. *Future Med Chem* 2013;5:2103–2116.
 20. Pickart MA, Klee EW. Zebrafish approaches enhance the translational research tackle box. *Transl Res* 2014;163:65–78.
 21. Howe K, Clark MD, Carlos F, Torroja CF, *et al.* The zebrafish reference genome sequence and its relationship to the human genome. *Nature* 2013;496:498–503.
 22. Brown AP, Chung EJ, Urlick ME, Shield WP, 3rd, Sowers AL, Thetford A, *et al.* Evaluation of the fullerene compound DF-1 as a radiation protector. *Radiat Oncol* 2010;11:34.
 23. Shin HA, Shin YS, Kang SU, Kim JH, Oh YT, Park KH, *et al.* Radioprotective effect of epicatechin in cultured human fibroblasts and zebrafish. *J Radiat Res* 2014;55:32–40.
 24. Epperly MW, Bahary N, Quader M, Dewald V, Greenberger JS. The zebrafish-*Danio rerio* is a useful model for measuring the effects of small-molecule mitigators of late effects of ionizing irradiation. *In Vivo* 2012;26:889–897.
 25. Chong CR, Chen X, Shi L, Liu JO, Sullivan DJ. A clinical drug library screen identifies astemizole as an antimalarial agent. *Nat Chem Biol* 2006;2:415–416.
 26. O'Boyle NM, Banck M, James CA, Morley C, Vandermeersch T, Hutchison GR. Open Babel: an open chemical toolbox. *J Cheminfo* 2011;3:33.
 27. Garg A, Tewari R, Raghava GPS. Virtual Screening of potential drug-like inhibitors against Lysine/DAP pathway of *Mycobacterium tuberculosis*. *BMC Bioinfo* 2010;10:1471–2105.
 28. Trott O, Olson AJ. AutoDock Vina: improving the speed and accuracy of docking with a new scoring function, efficient optimization and multithreading. *J Comp Chem* 2010;31:455–461.
 29. Chang MW, Ayeni C, Breuer S, Torbett BE. Virtual screening for HIV protease inhibitors: a comparison of AutoDock 4 and Vina. *PLoS One* 2010;5:e11955.
 30. Westerfield M: *The Zebrafish Book: A Guide for Laboratory Use of Zebrafish *Danio rerio**, 3rd ed. University of Oregon Press, Eugene, OR, 1994.
 31. Abdelkader TS, Chang SN, Kim TH, Song J, Kim DS, Park JH. Exposure time to caffeine affects heartbeat and cell damage-related gene expression of zebrafish *Danio rerio* embryos at early developmental stages. *J Appl Toxicol* 2012;10:2787.
 32. Ransom DG, Haffter P, Odenthal J, Brownlie A, Vogelsang E, Kelsh RN, *et al.* Characterization of zebrafish mutants with defects in embryonic hematopoiesis. *Development* 1996;123:311–319.
 33. Gardiner MR, Gongora MM, Grimmond SM, Perkins AC. A global role for zebrafish *klf4* in embryonic erythropoiesis. *Mech Dev* 2007;124:762–774.
 34. Livak JL, Schmittgen TD. Analysis of relative gene expression data using real-time quantitative PCR and the $2^{-\Delta\Delta C_T}$ method. *Methods* 2001;25:402–408.
 35. Ganis JJ, Hsia N, Trompouki E, de Jong JLO, DiBiase A, Lambert JS, *et al.* Zebrafish globin switching occurs in two developmental stages and is controlled by the LCR. *Dev Biol* 2012;366:185–194.
 36. Kishi S, Bayliss PE, Uchiyama J, Koshimizu E, Qi J, Nanjappa P, *et al.* The identification of zebrafish mutants showing alterations in senescence-associated biomarkers. *PLoS Genet* 2008;4:e1000152.
 37. Halliwell B, Gutteridge JMC, Aruoma OI. The deoxyribose method: a simple “test-tube” assay for determination of rate constants for reactions of hydroxyl radical. *Anal Biochem* 1987;165:215–219.
 38. del Toro R, Méndez-Ferrer SM. Autonomic regulation of hematopoiesis and cancer. *Haematologica* 2013;98:1663–1666.
 39. Wishart DS, *et al.* Drug Bank: a comprehensive resource for *in silico* drug discovery and exploration. *Nucleic Acids Res* 2006;34:D668–D672.
 40. Mohr AM, ElHassan IO, Hannoush EJ, Sifri ZC, Offin MD, *et al.* Does beta blockade postinjury prevent bone marrow suppression? *J Trauma* 2011;70:1043–1049.
 41. Baranski GM, Pasupuleti LV, Sifri ZC, Cook KM, Alzate WD, Rameshwar P, *et al.* Beta blockade protection of bone marrow following injury: a critical link between heart rate and immunomodulation. *J Bone Marrow Res* 2013;1:124.
 42. Cherezov V, *et al.* High-resolution crystal structure of an engineered human β_2 -adrenergic G protein-coupled receptor. *Science* 2007;318:1258–1265.
 43. Rosenbaum DM, *et al.* GPCR engineering yields high-resolution structural insights into β_2 -adrenergic receptor function. *Science* 2007;318:1266–1273.
 44. Kolba P, Rosenbaum DM, Irwina JJ, Fung J, Kobilka BK, Shoichet BK. Structure-based discovery of β_2 -adrenergic receptor ligands. *Proc Natl Acad Sci U S A* 2009;21:6843–6848.
 45. Berger J. Phenylhydrazine haematotoxicity. *J Appl Biomed* 2007;5:125–130.
 46. Kulkeaw K, Sugiyama D. Zebrafish erythropoiesis and the utility of fish as models of anemia. *Stem Cell Res Ther* 2012;3:55.
 47. Bauer A, Tronche F, Wessely O, Kellendonk C, Reichardt HM, Steinlein P, *et al.* The glucocorticoid receptor is required for stress erythropoiesis. *Genes Dev* 1999;13:2996–3002.
 48. Takizawa H, Schanz U, Manz MG. *Ex vivo* expansion of hematopoietic stem cells: mission accomplished? *Swiss Med Wkly* 2011;141:w13316.
 49. Ferri-Lagneau KF, Moshal KS, Grimes M, Zahora B, Lishuang L, Sang S, *et al.* Ginger stimulates hematopoiesis via Bmp pathway in zebrafish. *PLoS One* 2012;7:e39327.
 50. Long Q, Meng A, Wang H, Jessen JR, Farrell MJ, Lin S. GATA-1 expression pattern can be recapitulated in living transgenic zebrafish using GFP reporter gene. *Development* 1997;124:4105–4111.

51. Jin H, Sood R, Xu J, Zhen F, English MA, Liu PP, *et al.* Definitive hematopoietic stem/progenitor cells manifest distinct differentiation output in the zebrafish VDA and PBI. *Development* 2009;136:647–654.
52. Falenta K, Rodaway A. Definitive erythropoiesis in the trunk of zebrafish embryos. *Development* 2011;138:3861–3862.
53. Huang HT, Zon LI. Regulation of stem cells in the zebrafish hematopoietic system. *Cold Spring Harb Symp Quant Biol* 2008;73:111–118.
54. Geiger GA, Parker SE, Beothy AP, Tucker JA, Mullins MC, Kao GD. Zebrafish as a “Biosensor”? Effects of ionizing radiation and amifostine on embryonic viability and development. *Cancer Res* 2006;66:8172–8181.
55. Duffy KT, Wickstrom E. Zebrafish tp53 knockdown extends the survival of irradiated zebrafish embryos more effectively than the p53 inhibitor Pifithrin- α . *Cancer Biol Ther* 2007;6:675–678.
56. Daroczi B, Kari G, McAleer MF, Wolf JC, Rodeck U, Dicker AP. *In vivo* radioprotection by the fullerene nanoparticle DF-1as assessed in a zebrafish model. *Clin Cancer Res* 2006;12:7086–7091.
57. Djanani A, Kaneider NC, Meierhofer C, Sturn D, Duzendorfer S, Allmeier H, *et al.* Inhibition of neutrophil migration and oxygen free radical release by metipranolol and timolol. *Pharmacology* 2003;68:198–203.
58. Gasiorowski K, Brokos B. Evaluation of antimutagenic effect of todralazine in cultured lymphocytes. *Mutagenesis* 2000;15:137–141.
59. Parnig C, Anderson N, Ton C, McGrath P. Zebrafish apoptosis assays for drug discovery. *Methods Cell Biol* 2004;76:75–85.
60. Flesch M, Maack C, Cremers B, Bäumer AT, Südkamp M, Böhm M. Effect of β -Blockers on free radical-induced cardiac contractile dysfunction. *Circulation* 1999;100:346–353.
61. Finna J, Huib M, Lib V, Lorenzia V, de la Paza N, Cheng SH, *et al.* Effects of propranolol on heart rate and development in Japanese medaka (*Oryzias latipes*) and zebrafish (*Danio rerio*). *Aquat Toxicol* 2012;122–123:214–221.
62. Keiser MJ, Setola V, Irwin HJ, Laggner C, Abbas AI, *et al.* Predicting new molecular targets for known drugs. *Nature* 2009;462:175–181.
63. Araki H, Baluchamy S, Yoshinaga K, Petro B, Petiwala S, *et al.* Cord blood stem cell expansion is permissive to epigenetic regulation and environmental cues. *Exp Hematol* 2009;37:1084–1095.
64. Murata K, Hamada M, Sugimoto K, Nakano T. A novel mechanism for drug-induced liver failure: inhibition of histone acetylation by hydralazine derivatives. *J Hepatol* 2007;46:322–329.

Address correspondence to:
Indracanti Prem Kumar, PhD
Radiation Biosciences Division
Institute of Nuclear Medicine and Allied Sciences
Defense Research and Development Organization
Brig SK Majumdar Road
Timarpur
Delhi 110054
India

E-mail: prem_indra@yahoo.co.in